

## Direct observation of stronger flux-line pinning of crossed compared to parallel linear defects

Th. Schuster and H. Kuhn

*Max-Planck-Institut für Metallforschung, Institut für Physik, Postfach 800665, D-70506 Stuttgart, Germany*

M. V. Indenbom\*

*Institut de Génie Atomique, Ecole Polytechnique Fédérale de Lausanne, CH-1015 Lausanne, Switzerland*

G. Kreiselmeyer and M. Leghissa†

*III. Physikalisches Institut, Universität Erlangen-Nürnberg, Erwin-Rommel-Strasse 1, D-91058 Erlangen, Germany*

S. Klaumünzer

*Hahn-Meitner-Institut, Postfach 390128, D-14091 Berlin, Germany*

(Received 14 August 1995)

Linear defects were introduced in high-temperature superconductors (HTSC's) by high-energy heavy-ion irradiation. Flux penetration into partly crossed and parallel irradiated HTSC's was observed by magneto-optics. The obtained flux distributions show that the critical current density  $j_c$  in cross-irradiated HTSC's is larger by a factor up to 14 than in parallel irradiated HTSC's.

The knowledge of the flux-line (FL) pinning and depinning mechanisms is particularly important for high-temperature superconductors (HTSC's) for both the improvement of their performance in technical applications and the theoretical understanding of type-II superconductivity.<sup>1</sup> To our present knowledge, the most effective pinning centers for FL's are linear defects (LD's), which can be introduced into HTSC's by high-energy heavy-ion irradiation.<sup>2</sup> LD's also allow features of the FL lattice to be investigated,<sup>3</sup> e.g., depinning processes or the differences between two- and three-dimensional FL's. In infinitely extended samples, depinning of FL's oriented parallel to the LD's can occur only by kink-pair nucleation in the volume as considered by Brandt<sup>4</sup> and in the statistical theory of thermal depinning from randomly distributed LD's (Bose-glass model).<sup>5</sup> In finite samples FL's can also depin by the nucleation of single kinks between two LD's at the sample surface, which requires a lower activation energy than the nucleation of kink pairs. These kinks slide along the LD's without pinning; see Fig. 1(a). The existence of the nucleation of single kinks at the sample surface is supported by recent experiments<sup>6,7</sup> on obliquely irradiated HTSC's. Investigations of FL's inclined to the LD's by a large angle are of particular interest if one wants to produce nonparallel LD's in order to increase  $j_c$  and the irreversibility temperature  $T_{irr}$  above that of LD's parallel to the FL's.<sup>7-9</sup>

For effective pinning the kinks have to be impeded from sliding along the LD's. This can happen at the sites where the distance between two nonparallel LD's is smallest. The kinks nucleate at the sample surface and slide the short distance until they are trapped between two crosswisely running LD's; see Fig. 1(b). For FL depinning from these traps three different depinning modes *A*, *B*, and *C* are considered [see Ref. 7 and Fig. 1(c)]. In mode *A*, thermal fluctuations depin the FL at the trap, such that the kink runs on a smooth curve, which shortens the acute angle between the two LD's; see Fig. 1(c). For sufficiently large fluctuations, the kink can reach a third LD and, when a section of the FL is pinned

there, the kink is split into a kink pair. Both kinks (of the kink pair) slide antiparallel along the LD's until they are trapped again between two nonparallel LD's at their smallest distance. Mode *B* is the well-known kink-pair nucleation as considered in Refs. 4 and 5, which occurs for flux motion when FL's and LD's are parallel to each other. Because of the different geometrical arrangements of FL's and LD's, mode *A* has a lower activation energy than mode *B*. At the obtuse angle in mode *C* depinning occurs similarly to mode *A*, but now the FL must be stretched to extend the kink towards the next LD in the direction of flux motion, which requires a higher activation energy than mode *A*. Therefore, mode *C* can safely be excluded in the following considerations. The difference between the depinning modes *A* and *B* was revealed by magneto-optic observations of the anisotropic flux penetration in cross-irradiated DyBa<sub>2</sub>Cu<sub>3</sub>O<sub>7- $\delta$</sub>  (DBCO) crystals.<sup>6,7</sup> The measured ratio of the pinning forces of modes *A* and *B* is between 1.1 at low  $T$ 's and 2.3 near the superconducting transition temperature  $T_c$ . This strongly indicates that FL motion in DBCO occurs because of the two different depinning modes *A* and *B*. In Bi<sub>2</sub>Sr<sub>2</sub>CaCu<sub>2</sub>O<sub>8+ $\delta$</sub>  (Bi2212) such a difference was not observed.<sup>7</sup> This result was attributed to the pancake structure of the FL's in Bi2212.

In the present paper we show directly that crossed LD's are more effective pinning sites than parallel LD's. As shown in a recent paper<sup>10</sup> magneto-optics provide an extremely sensitive tool to study spatial variations of the critical current density  $j_c$ . We introduced crossed LD's in only one-half of each sample. The other regions of the samples were then irradiated perpendicular to the sample surface. We present local observations of the qualitatively different flux penetration in both parts of one sample, thus avoiding the influence of the large scatter in the quality of HTSC's on our results. The magneto-optically detectable difference in  $j_c$  may be even smaller than a  $j_c$  inhomogeneity in each part of the sample before irradiation.

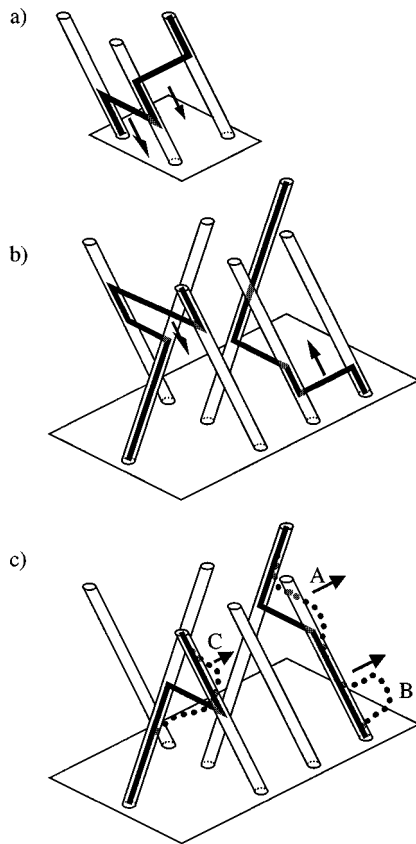


FIG. 1. Sketch of FL motion in the presence of parallel and crossed LD's. The directions of FL and kink motion are indicated by arrows. The FL's are the bold lines; the LD's are sketched as oblique cylinders. Hidden FL segments are plotted in grey. (a) The kinks (segments of the FL's between two LD's), which are nucleated at the sample surface, slide along parallel LD's. (b) The kinks of the FL's slide along the LD's until they are trapped at the smallest distance between two nonparallel LD's. (c) The kinks are now trapped and run between the nonparallel LD's. The FL's are thermally depinned by different activation processes labeled A, B, and C as indicated. The run of the depinned kinks is indicated by the dotted lines.

Our single crystals of DBCO were prepared with  $T_c = 91$  K and a transition width  $\Delta T_c = 1$  K by a self-flux method as described in Ref. 11. The preparation route of the Bi2212 single crystals is given in Ref. 12. The obtained crystals had  $T_c = 88$  K and  $\Delta T_c = 2.2$  K. The sample thickness was about  $15 \mu\text{m}$  for the DBCO crystals and about  $20 \mu\text{m}$  for the Bi2212 crystals.

LD's were produced by irradiating the samples at room temperature with 500-MeV Xe ions at the Hahn-Meitner-Institut in Berlin, Germany. The range of this projectile also exceeds the thickness of the samples for oblique irradiation. The sample holder can be fixed on the mounting plate at the three angles  $\varphi = 0^\circ$ ,  $+45^\circ$ , and  $-45^\circ$ ; see Fig. 2(a). During the irradiation, one-half of each sample was covered by a 500- $\mu\text{m}$ -thick aluminum absorber in order to allow both parts to be irradiated independently from each other. The absorber can be rotated by  $180^\circ$  as indicated by the arrow in Fig. 2(b). With this sample holder we irradiated one half of each sample perpendicular to the sample surface ( $\varphi=0^\circ$ ). Subsequently we introduced crossed LD's in the other part

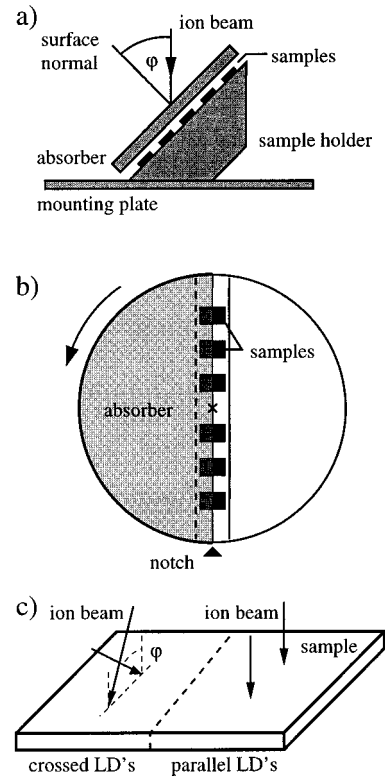


FIG. 2. Sketch of the sample holder and the irradiation arrangement. (a) A cross section of the sample holder mounted for irradiation at  $\varphi = 45^\circ$ . (b) A plan view of the sample holder. The edge of the absorber is located exactly on the diameter. Only one-half of each sample is exposed to the ion beam. To expose the covered part of the samples to the ion beam, the absorber can be rotated as indicated by the arrow. The exact position of the absorber is ensured by a notch. (c) Sketch of the ion-beam direction with respect to the sample.

( $\varphi = \pm 45^\circ$ ). For each angle setting ( $\varphi = +45^\circ$  and  $-45^\circ$ ) we irradiated the sample to half the fluence as used for perpendicular irradiation, such that the total fluence  $\phi t = 1 \times 10^{10} \text{ cm}^{-2}$  is the same for both parts. During the crossed irradiation the incident ion beam was directed along the absorber edge to ensure that the produced LD's do not extend into the perpendicular irradiated sample part; see Fig. 2(c). The edge of the absorber is justified exactly on the diameter of the sample holder, such that the differently irradiated parts do not overlap or are separated by an unirradiated zone. Since the fluence is measured for a perpendicular cross section of the ion beam, we have a lower number of defects per unit area (measured parallel to the sample surface) in the obliquely irradiated parts of the samples, but the LD's are longer. Thus the damaged volume, which is the relevant parameter for a comparison of  $j_c$ , is equal in both parts. A homogeneous defect density was achieved by waving the ion beam over the sample surface. The heavy-ion irradiation reduces  $T_c$  by about 0.5 K at the fluence used.

To visualize the magnetic flux distribution we use the magneto-optical Faraday effect in ferrimagnetic garnet films with an in-plane anisotropy. The full description of this technique is given in Ref. 13. This technique allows us to observe flux distributions in the whole temperature range  $5 \text{ K} \leq T \leq T_c$  with a spatial resolution of about  $3 \mu\text{m}$ . The lower

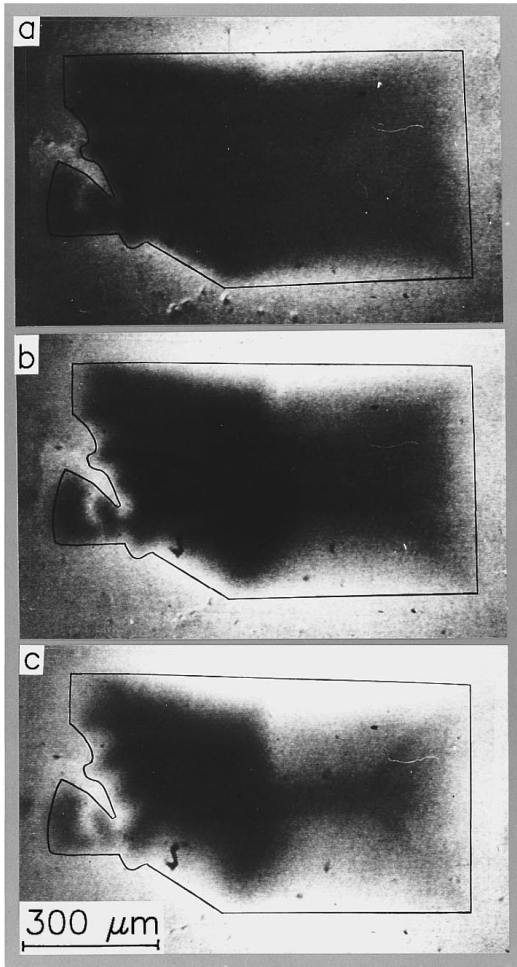


FIG. 3. Flux distribution in a DBCO single crystal after irradiation with 500-MeV Xe ions. Crossed LD's were introduced only into the left part of the sample, whereas the right part contains parallel LD's. The magnetic field  $H_a$  is applied perpendicular to the sample surface and the observation temperature is 50 K. (a)  $\mu_0 H_a = 43$  mT, (b) 85 mT, and (c) 128 mT.

temperature limit is given by the cryostat used.<sup>14</sup>

To discuss our results, we choose one DBCO single crystal, which exhibits a typical behavior of our numerous samples before and after irradiation. Figure 3 shows the flux penetration into a partly crossed and parallel irradiated DBCO single crystal in perpendicular magnetic fields of  $\mu_0 H_a = 85$  mT (a), 171 mT (b), and 256 mT (c) at  $T = 50$  K. The bright areas represent the Shubnikov phase into which FL's have already penetrated, whereas the flux-free Meissner phase remains dark. The black frame marks the sample edges. Crossed LD's ( $\varphi = \pm 45^\circ$ ) were introduced only into the left part of the sample, whereas the right part contains parallel LD's oriented perpendicular to the sample surface as sketched in Fig. 2(c). The boundary between the two parts runs perpendicular to the upper sample edge starting from its center. The deeper flux penetration into the right part of the sample as compared to the cross-irradiated left part shows that the critical current density  $j_c$  is more strongly enhanced by crossed LD's than by parallel ones ( $j_c^p$ ). In Fig. 3(c) the critical state, i.e., complete flux penetration is reached in the parallel irradiated part of the sample, whereas a large Meissner phase remains in the cross-irradiated region.

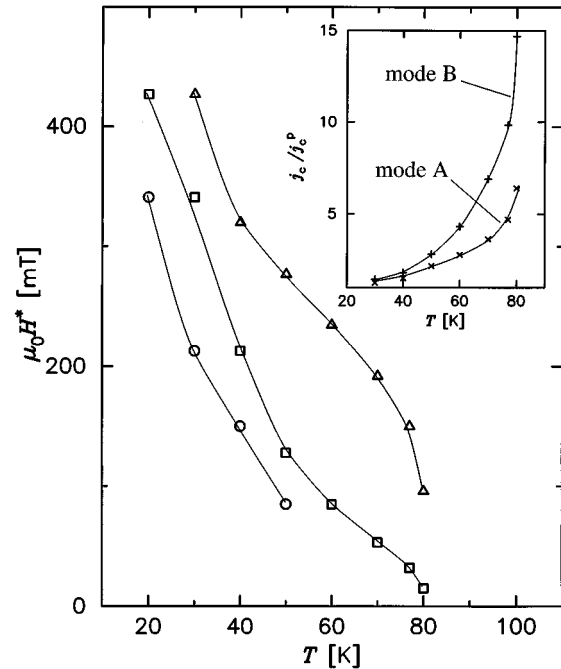


FIG. 4. Temperature dependence of the full penetration field  $H^*$  of unirradiated (O), parallel irradiated (□), and cross-irradiated (△) DBCO. The inset shows the temperature dependence of the ratio  $j_c/j_c^p$ . (×) is  $j_c$  limited by depinning mode A. (+) is  $j_c$  caused by depinning mode B.

From the external magnetic field  $H^* = (j_c d/2) \ln(4a/d)$  (thickness  $d$ , half width  $a$ ), when the differently irradiated regions are just completely penetrated by flux, we can deduce the ratio of the lower  $j_c$  (depinning mode A) in the cross-irradiated region and  $j_c^p$ . The ratio of the larger (depinning mode B) and the lower  $j_c$  (depinning mode A) in the cross-irradiated part can be determined from the flux distribution when the cross-irradiated sample part is in the critical state.<sup>10</sup> In Fig. 4 the temperature dependence of  $H^*$  is plotted for the unirradiated crystal (O), the parallel irradiated (□), and the cross-irradiated (△) part of the sample. Note that  $H^*$  for the cross-irradiated part is determined by the depinning mode A. From the increase of  $H^*$  caused by irradiation at a given temperature we can conclude that the critical current density is enhanced. For example, at  $T = 50$  K,  $j_c$  is enhanced from  $1.7 \times 10^5$  A/cm<sup>2</sup> by a factor of 1.5 because of parallel irradiation and even by a factor of 3.5 because of crossed irradiation. The inset shows the ratio  $j_c/j_c^p$  versus temperature for depinning mode A (×) determined from the  $H^*$  values and for depinning mode B (+). The temperature behavior of  $j_c/j_c^p$  indicates that the activation energy in the cross-irradiated part of the sample is larger than the activation energy in the parallel irradiated region. As stated above, the different activation energies are caused by the different depinning processes by kink-pair and surface-kink nucleation. The ratio  $j_c/j_c^p$  for depinning mode A can also be determined from the flux distribution in the critical state.<sup>10</sup> These values nicely agree with the data plotted in the inset in Fig. 4.

The same experiments were performed with partly crossed and parallel irradiated Bi2212 single crystals. Because of the pancake structure of the FL's, we cannot observe

the different depinning modes *A* and *B* in the cross-irradiated sample parts. We found that the ratio of the critical currents in both sample parts  $j_c/j_c^p \approx 1.5$  is temperature independent in the range  $5 \text{ K} \leq T \leq 80 \text{ K}$ . Therefore, we conclude that flux motion proceeds by depinning of single pancake vortices, which requires the same activation energy for parallel and crossed LD's. The difference between the critical current densities in both sample parts is then because of the geometrical arrangement of the LD's. For parallel LD's the pancake vortices can depin at every place along the LD. One depinning event is then enough to move all pancakes to the next LD. For crossed LD's the vortices depin preferentially at the crossover of two nonparallel LD's. In this case, many more depinning events than for parallel LD's must occur for a real FL motion. The factor of 1.5 between the two critical current densities flowing in both sample parts should be obtained from statistical considerations.

In summary, by magneto-optics we observed flux penetration into partly crossed and parallel irradiated DBCO and Bi2212 single crystals. We have shown that FL's are more strongly pinned by crossed LD's than by parallel ones. In

DBCO the ratio of the critical current densities flowing in the parallel and crossed irradiated sample parts increases with temperature from unity up to about 6 for depinning mode *A* and up to a factor of about 14 for depinning mode *B*. This finding is attributed to the different depinning processes by single-kink nucleation at the sample surface in the presence of parallel LD's and by kink-pair nucleation in the presence of crossed LD's. In Bi2212 we found that the ratio  $j_c/j_c^p \approx 1.5$  is temperature independent in the range  $5 \text{ K} \leq T \leq 80 \text{ K}$ . This was attributed to equal activation energies in both sample parts.

We thank H. Kronmüller and G. Saemann-Ischenko for their constant interest in this work, the Bundesministerium für Bildung, Wissenschaft, Forschung und Technologie (Grant No. 13N6510) and the Bayerischer Forschungsverbund Hochtemperatur-Supraleiter FORSUPRA for financial support, and T. W. Li and the Dutch FOM (ALMOS) for the Bi2212 single crystals. One of us (M.V.I.) is grateful to the Swiss National Foundation for financial support under Grant No. PNR 4030-32794.

\*Permanent address: Institute of Solid State Physics, Russian Academy of Science, 142432 Chernogolovka, Russia.

†Permanent address: Siemens AG, Zentrale Forschung und Entwicklung ZFE T EP 4, Postfach 3220, D-91050 Erlangen, Germany.

<sup>1</sup>S. Senoussi, *J. Phys. (France) III* **2**, 1041 (1992).

<sup>2</sup>L. Civale, A. D. Marwick, T. K. Worthington, M. A. Kirk, J. A. Thompson, L. Krusin-Elbaum, Y. Sun, J. R. Clem, and F. Holtzberg, *Phys. Rev. Lett.* **67**, 648 (1991); M. Konczykowski, F. Rullier-Albenque, E. R. Yacobi, A. Shaulov, Y. Yeshurun, and P. Lejay, *Phys. Rev. B* **44**, 7167 (1991); V. Hardy, J. Provost, D. Groult, M. Hervieu, B. Raveau, S. Durcok, E. Pollert, J. C. Frison, J. P. Chaminade, and M. Pouchard, *Physica (Amsterdam) C* **201**, 85 (1992); M. Leghissa, Th. Schuster, W. Gerhäuser, S. Klaumünzer, M. R. Koblichka, H. Kronmüller, H. Kuhn, H.-W. Neumüller, and G. Saemann-Ischenko, *Europhys. Lett.* **11**, 323 (1992); Th. Schuster, M. R. Koblichka, H. Kuhn, H. Kronmüller, M. Leghissa, W. Gerhäuser, G. Saemann-Ischenko, H.-W. Neumüller, and S. Klaumünzer, *Phys. Rev. B* **46**, 8496 (1992); Th. Schuster, M. Leghissa, M. R. Koblichka, H. Kuhn, H. Kronmüller, and G. Saemann-Ischenko, *Physica (Amsterdam) C* **203**, 203 (1992).

<sup>3</sup>W. Gerhäuser, G. Ries, H.-W. Neumüller, W. Schmitt, O. Eibl, G. Saemann-Ischenko, and S. Klaumünzer, *Phys. Rev. Lett.* **68**, 879 (1992).

<sup>4</sup>E. H. Brandt, *Europhys. Lett.* **18**, 635 (1992); *Phys. Rev. Lett.* **69**, 1105 (1992).

<sup>5</sup>D. R. Nelson and V. M. Vinokur, *Phys. Rev. Lett.* **68**, 2389 (1993); *Phys. Rev. B* **48**, 13 060 (1993).

<sup>6</sup>Th. Schuster, M. V. Indenbom, H. Kuhn, H. Kronmüller, M. Leghissa, and G. Kreiselmeyer, *Phys. Rev. B* **50**, 9499 (1994).

<sup>7</sup>Th. Schuster, H. Kuhn, M. V. Indenbom, M. Leghissa, M. Kraus, and M. Konczykowski, *Phys. Rev. B* **51**, 16 358 (1995).

<sup>8</sup>T. Hwa, P. Le Doussal, D. R. Nelson, and V. M. Vinokur, *Phys. Rev. Lett.* **71**, 3545 (1993).

<sup>9</sup>L. Civale, L. Krusin-Elbaum, J. R. Thompson, R. Wheeler, A. D. Marwick, M. A. Kirk, Y. R. Sun, F. Holtzberg, and C. Feild, *Phys. Rev. B* **50**, 4102 (1994); L. Krusin-Elbaum, J. R. Thompson, R. Wheeler, A. D. Marwick, C. Li, S. Patel, D. T. Shaw, P. Lisowski, and J. Ullmann, *Appl. Phys. Lett.* **64**, 3331 (1994); G. Kreiselmeyer, M. Müller, M. Kraus, B. Holzapfel, S. Bouffard, and G. Saemann-Ischenko, *Physica (Amsterdam) C* **235-240**, 3056 (1994).

<sup>10</sup>Th. Schuster, M. V. Indenbom, M. R. Koblichka, H. Kuhn, and H. Kronmüller, *Phys. Rev. B* **49**, 3443 (1994).

<sup>11</sup>C. Thomsen, M. Cardona, B. Gegenheimer, R. Liu, and R. Simon, *Phys. Rev. B* **37**, 9860 (1988).

<sup>12</sup>T. W. Li, P. H. Kes, N. T. Hien, J. J. M. Franse, and A. A. Menovsky, *J. Cryst. Growth* **135**, 481 (1994).

<sup>13</sup>L. A. Dorosinskii, M. V. Indenbom, V. I. Nikitenko, Yu. A. Ossip'yan, A. A. Polyanskii, and V. K. Vlasko-Vlasov, *Physica (Amsterdam) C* **203**, 149 (1992).

<sup>14</sup>K.-H. Greubel, E. Gmelin, N. Moser, Ch. Mensing, and L. Walz, *Cryogenics* **30** (Suppl.), 457 (1990).